Received: 13 February 2023 | Revised: 2 August 2023 | Accepted: 28 August 2023

DOI: 10.1002/psp4.13042

ARTICLE

A multicompartment population PK model to predict tenofovir and emtricitabine mucosal tissue concentrations for HIV prevention

Erick Leung[1] | **Mackenzie L. Cottrell**[1] | **Craig Sykes**[1] | **Nicole White**[2] | **Angela D. M. Kashuba**[1,2] | **Julie B. Dumond**[1]

[1]Division of Pharmacotherapy and Experimental Therapeutics, University of North Carolina UNC Eshelman School of Pharmacy, Chapel Hill, North Carolina, USA

[2]University of North Carolina School of Medicine, Chapel Hill, North Carolina, USA

Correspondence
Julie B. Dumond, Division of Pharmacotherapy and Experimental Therapeutics, UNC Eshelman School of Pharmacy, University of North Carolina at Chapel Hill, 1093 Genetic Medicine Building, CB# 7361, 120 Mason Farm Road, Chapel Hill, NC 27599-7361, USA.
Email: jdumond@unc.edu

Present address
Erick Leung, Certara, Inc., Princeton, New Jersey, USA

Funding information
National Institute of Allergy and Infectious Diseases, Grant/Award Number: U01AI09503; Centers for AIDS Research, Grant/Award Number: CFAR P30 AI50410; National Institute of General Medical Sciences, Grant/Award Number: 5T32GM086330

Abstract

A priori use of mathematical modeling and simulation to predict outcomes from incomplete adherence or reduced frequency dosing strategies may mitigate the risk of clinical trial failure with HIV pre-exposure prophylaxis regimens. We developed a semi-physiologic population pharmacokinetic model for two antiretrovirals and their active intracellular metabolites in three mucosal tissues using pharmacokinetic data from a phase I, dose-ranging study. Healthy female volunteers were given a single oral dose of tenofovir disoproxil fumarate (150, 300, or 600 mg) or emtricitabine (100, 200, or 400 mg). Simultaneous co-modeling of all data was performed on a Linux cluster. A 16 compartment, bolus input, linear kinetic model best described the data, containing 986 observations in 23 individuals across three matrices and four analytes. Combined with a defined efficacious concentration target in mucosal tissues, this model can be used to optimize the dose and dosing frequency through Monte-Carlo simulations.

Study Highlights

WHAT IS THE CURRENT KNOWLEDGE ON THE TOPIC?

Tenofovir (TFV) disoproxil fumarate + emtricitabine (FTC) prevents sexual transmission of HIV in high-risk individuals. However, gender differences in adherence necessary for effectiveness are noted across clinical trials. This discrepancy is partially explained by differential drug distribution between mucosal tissue transmission sites.

WHAT QUESTION DID THIS STUDY ADDRESS?

Most pharmacokinetic models for HIV prevention do not allow investigators to simultaneously predict distribution of TFV, FTC, and their active metabolites (TFV-diphosphate [dp] and FTC-triphosphate [tp]) to vulnerable tissues; we sought this utility inform tissue pharmacokinetics under varying clinical scenarios.

WHAT DOES THIS STUDY ADD TO OUR KNOWLEDGE?

We developed an eight-compartment pharmacokinetic model for HIV prevention to simulate exposure of TFV, TFV-dp, FTC, and FTC-tp in cervical, vaginal, and rectal tissue. Our model parameters were validated with tissue data from a phase I, dose-ranging pharmacokinetic trial.

HOW MIGHT THIS CHANGE DRUG DISCOVERY, DEVELOPMENT, AND/OR THERAPEUTICS?

This model will predict drug exposure from variable adherence and alternative pre-exposure prophylaxis dosing. This approach can be paired with efficacy targets to predict clinical trial outcomes a priori, maximizing the chances of successful HIV prevention.

INTRODUCTION

A fixed dose combination tablet of tenofovir disoproxil fumarate (TDF) with emtricitabine (FTC) received US Food and Drug Administration (FDA) approval for HIV pre-exposure prophylaxis (PrEP) in 2012. However, clinical trials evaluating the efficacy of daily TDF with and without FTC for PrEP have demonstrated mixed results in women. Whereas the TDF and partners PrEP trials demonstrated 62%–75% efficacy,[1,2] the FEM-PrEP and VOICE trials found no difference between the study treatments and placebo.[3,4] Post hoc analysis of drug concentrations of TDF in plasma samples collected during the FEM-PrEP and VOICE trials revealed that less than 30% of women enrolled to the daily active treatment arms of oral TDF with and without FTC exhibited detectable drug concentrations despite adherence estimates from self-report and clinic based product count exceeding 85%.[3,4] Yet, for men who have sex with men (MSM), TDF with FTC demonstrates 76% protection if 28% of intended doses are taken.[5,6] This indicates that the adherence threshold for efficacy may differ between study populations. This remained an issue even in 2019 when the FDA approved a new formulation of tenofovir called tenofovir alafenamide (TAF) in combination with FTC as a second option for HIV PrEP. This approval was only given for MSM and trans women, but not for cisgender women who have receptive vaginal sex due to a lack of clinical evidence as well as evidence from the FEM-PrEP and VOICE trials indicating potential differences in efficacy between men and women using PrEP at the same frequency of adherence.

TDF is converted to tenofovir (TFV) in the plasma after absorption from the gastrointestinal (GI) tract, whereas TAF is converted to tenofovir predominately at its site of action in lymphocytes. Once in the active site, TFV and FTC are intracellularly phosphorylated into their pharmacologically active moieties, TFV diphosphate (TFVdp) and FTC triphosphate (FTCtp). Although several published pharmacokinetic models describe the distribution of these compounds in the blood of people living with HIV,[7–10] our goal was to develop a model in people not living with HIV that improved upon existing models[11–15] by incorporating mucosal tissue compartments and concentrations of FTC and FTCtp along with TFV and TFVdp. Because pharmacokinetic-pharmacodynamic modeling and simulation is commonly used by the pharmaceutical industry to streamline the drug development process by optimizing the dosing regimens selected for phase II and III trials,[16,17] such a model could be used a priori in the HIV PrEP field to identify the impact of various adherence scenarios or determine the efficacy of intermittent dosing strategies. Therefore, the objective of this study was to develop and qualify a population pharmacokinetic model to describe the plasma and mucosal tissue pharmacokinetics of TFV, FTC, and their active metabolites in people living without HIV.

METHODS

Trial design

Pharmacokinetic data obtained from a previously published phase I, open-label, dose ranging study[18] was used to build the model. Forty-nine healthy, premenopausal women gave informed consent before receiving a single oral dose of TDF (150, 300, or 600 mg) or FTC (100, 200, or 400 mg). Blood was intensively sampled at baseline and over 48 h for drug concentration quantification in plasma. Each participant provided one cervical, vaginal, and rectal tissue sample at 6, 12, 24, or 48 h postdose. The clinical trial protocol was registered with ClinicalTrials.gov (NCT01330199) and all study procedures were conducted in accordance with Good Clinical Practice, approved by

the University of North Carolina's Biomedical Institutional Review Board, and adhered to the ethical standards of the responsible committee on human experimentation and with the Helsinki Declaration of 1975 (as revised in 1983).

Population PK model

Nonlinear mixed effects fitting was performed with NONMEM 7.3 (ICON, plc) using FOCE-I on a Linux computing cluster with parallelization. Pre and post-processing was done with R[19] using libraries ggplot2,[20] dplyr,[21] tidyr,[22] and xpose.[23] Base plasma models for both TDF and FTC were developed through testing one and two compartment models with guidance from previous published literature.[7–12] To obtain the base tissue model, we fixed the plasma PK parameter values of TFV and FTC, then included the tissue concentration data of TFV, FTC, and their metabolites and fixed the values of tissues volumes of distribution equal to the tissue volumes accessed physiologically based as follows: rectal tissue volume was fixed to 0.17 L, assuming tissue density 1 g/mL: mean rectum length/colon length (11/135) = 0.08; 0.08 × 4.5 pounds (colon weight) = 170 g. Similarly, the cervix and uterus together weigh 70 g, with the bulk of the weight being the uterine body and lower uterine segment. The cervix alone was estimated to be 10 g. Finally, vaginal tissue was estimated to be 90 g. In addition to tissue volumes, we implemented a gut transit delay component[24] to describe drug distribution to the rectal tissue. Units were converted to nmol/L for model fitting, assuming tissue density of 1 g/mL. All fitted parameters were then used as initial estimates for simultaneously co-modeling both plasma and metabolite concentrations.

Baseline demographic covariate modeling was not performed due to homogeneity of the population shown in Table S1, and the model was assumed to be linear. Model diagnostics were performed with prediction-corrected visual predictive checks (pcVPCs) and goodness of fit plots. Monte-Carlo Simulations of 1000 replicates were performed on the dataset comprising of the three dosing levels: 50%, 100%, and 200% of the licensed treatment dose. The results were then normalized to 100% of the clinical dose group for the pcVPC.[25] The 95% confidence interval (CI) (bias-corrected and accelerated) around the prediction intervals were calculated by performing 1000 sets of bootstraps of the simulated concentrations using Pearl speaks NONMEM on a Linux-based computing cluster.[26,27] Difficult to estimate model parameters were fixed as denoted in Table 1. Within sample residual error correlations were also taken into account for measurements taken at the same time.

Analytical methods

Plasma samples were analyzed for TFV and FTC concentrations by a validated liquid chromatography/tandem mass spectrometry (LC–MS/MS) assay. The calibration range for the assay is 5–5000 ng/mL, and precision and accuracy were within 15% coefficient of variation (CV). Tissue samples were analyzed for TFV, FTC, TFVdp, FTCtp, deoxyadenosine triphosphate, and deoxycytidine triphosphate concentrations by a validated LC–MS/MS assay. The calibration range for the assay is 0.02–20 ng/mL homogenate. The blank matrix for this assay was human tissue homogenate. Precision and accuracy were within 20% CV. Detailed analytical methods have been previously published in the supplemental materials of ref. 18.

RESULTS

There were 23 individuals with 413 observations in the TFV dataset (275 plasma, 23 TFV, and 23 TFVdp in vaginal, cervical, and rectal tissue each) and 573 observations in the FTC dataset (276 plasma, 22 FTC, and 22 FTCtp in vaginal tissue and 23 FTC and 23 FTCtp in cervical and rectal tissue each). For TFV, seven, eight, and eight patients received doses of 150, 300, and 600 mg respectively, and for FTC, eight, seven, and eight patients received doses of 100, 200, and 400 mg, respectively.

A two-compartment model was found to best describe plasma kinetics for both TFV and FTC before subsequently incorporating mucosal tissues. These estimated parent drug parameters were fixed before modeling the parent and metabolite data simultaneously (Figure 1). Refinements made to this model that resulted in better fits to parameters include the addition of a seven-compartment gut transit model to better describe a delayed second peak in rectal tissue concentrations as well as removal of inter-individual variability (IIV) in metabolite clearance. It was assumed that the clearance of parent drug from tissues is due to loss in mucosal secretions, whereas clearance of drug metabolite is due to normal catabolic pathways of immune cells in the tissue as phosphorylation will trap the metabolite in the cell. Vaginal tissue volumes (Vv, Vvtp) were fixed to 0.09 L, cervical (Ve, Vetp) to 0.01 L, and rectal (Vr, Vrtp) to 0.17 L. This was estimated by taking account of physiologically relevant parameters, as mentioned in the Methods.

TABLE 1 Final estimated parameters and associated interindividual and residual variabilities.

Parameter (units)	Final estimate FTC	Final estimate TFV
K_a (1/h)	0.649	0.863
V_c (L)	72.3	331
V_p (L)	122	843
Q (L/h)	6.06	142
CL_{tt} (L/h)	18.9	58.7
Fv (fraction, $\times 10^{-5}$)	131	7.90
Fe (fraction, $\times 10^{-5}$)	6.90	1.50
Fr (fraction, $\times 10^{-5}$)	401	7.00
Fvt (fraction)	0.325	0.243
CL_{ttvvtp} (L/h)	0101	0.0111
CL_{vvtp} (L/h)	0.0399	0.0410
Fet (fraction)	1.00[a]	0.0292
CL_{ttve} (L/h, $\times 10^{-3}$)	0.947	1.83
CL_{vetp} (L/h, $\times 10^{-3}$)	8.2	2.07
Frt (fraction)	0.0107	1.00[a]
CL_{ttvr} (L/h, $\times 10^{-3}$)	22.3	4.77
CL_{vrtp} (L/h)	0.647	0.140
K_g (1/h)	0.0724	0.0752
K_{ga} (1/h)	1.00[a]	0.0589
K_{gr} (1/h)	1.00[a]	1.00[a]
ω on K_a, %CV (%shrinkage)	51.7 (17.4)	37.7 (18.9)
ω on V_c, %CV (%shrinkage)	20.5 (27.2)	39.0 (11.6)
ω on CL_{ttvvtp}, %CV (%shrinkage)	38.3 (14.9)	–
ω on CL_{tt}, %CV (%shrinkage)	–	22.7 ([b]V_c 100; 11.5)
ω on CL_{vvtp}, %CV (%shrinkage)	39.9 (42.6)	97.6 (1.0×10^{-10})
ω on CL_{ttve}, %CV (%shrinkage)	34.4 (27.1)	–
ω on CL_{vetp}, %CV (%shrinkage)	164.9 (4.69)	172 (0.889)
ω on CL_{ttvr}, %CV (%shrinkage)	87 (15.0)	–
ω on K_g, %CV (%shrinkage)	70.1 (15.6)	87.8 (17.3)
σ on Parent drug in plasma (%CV)	31.6	28.4
σ on Parent drug in vaginal compartment (%CV)	24.2	39.1
σ on Metabolite in vaginal compartment (%CV)	83.1 ([b]−9.27, parent)	42.3 ([b]99.6, parent)
σ on Parent drug in cervical compartment (%CV)	66.9	42.0
σ on Metabolite in cervical compartment (%CV)	58.2 ([b]96.3, parent)	31.1 ([b]98.9, parent)
σ on Parent drug in rectal compartment (%CV)	1.51	51.3
σ on Metabolite in plasma (%CV)	81.9 ([b]1.39, parent)	56.5 ([b]−20.0, parent)

Abbreviations: %CV, coefficient of variation in percentage terms; CL_{tt}, rate of total drug clearance; CL_{ttve}, clearance rate of drug from cervical compartment; CL_{ttvr}, clearance rate of drug from rectal compartment; CL_{ttvvtp}, clearance rate of drug from vaginal compartment; CL_{vetp}, clearance rate of metabolite from cervical compartment; CL_{vrtp}, clearance rate of metabolite from rectal compartment; CL_{vvtp}, clearance rate of metabolite from vaginal compartment; Fe, fraction of drug partitioned into cervical compartment; Fet, fraction of drug converted into metabolite in cervical compartment; Fr, fraction of drug partitioned into rectal compartment; Frt, fraction of drug converted into metabolite in rectal compartment; FTC, emtricitabine; Fv, fraction of drug partitioned into vaginal compartment; Fvt, fraction of drug converted into metabolite in vaginal compartment; K_a, absorption rate constant; K_g, transit rate; K_{ga}, transfer rate of drug from gut to rectal compartment; K_{gr}, elimination rate of drug from gut; Q, flow rate; TFV, tenofovir; V_c, ventral compartment volume; V_p, peripheral compartment volume; σ (sigma), residual variability; ω (omega), interindividual variability.

[a]Fixed.

[b]Off diagonals.

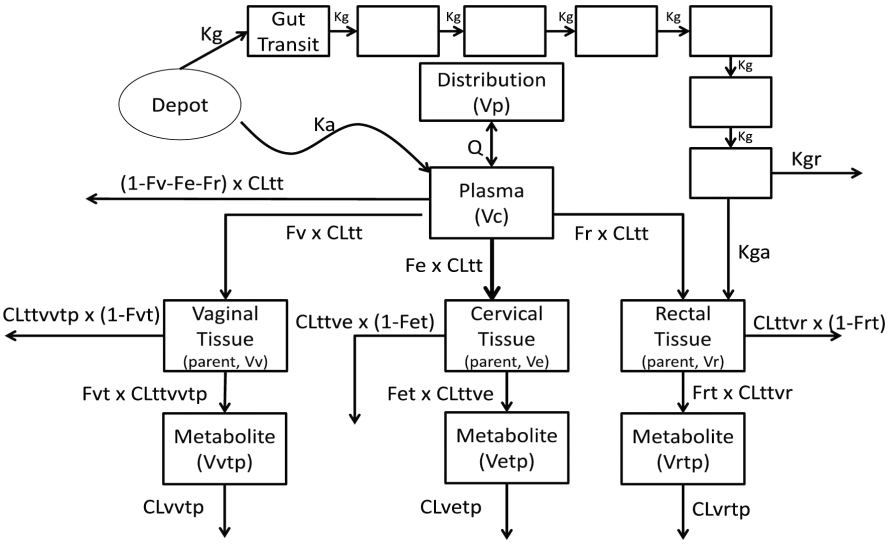

FIGURE 1 Structural model is linear with first-order absorption from gut into the plasma, and seven transit compartments for gut tissue.

The following describes the basic structure of the system:

$$\frac{dX_{plasma}}{dt} = K_a \times X_{depot} - \frac{Q}{V_c} \times X_{plasma} + \frac{Q}{V_p} \times X_{peripheral} - \frac{CL_{tt} \times (1 - Fv - Fe - Fr)}{V_c} \times X_{plasma} - \frac{CL_{tt} \times Fv}{V_c} \times X_{plasma} - \frac{CL_{tt} \times Fe}{V_c} \times X_{plasma} - \frac{CL_{tt} \times Fr}{V_c} \times X_{plasma} \quad (1)$$

$$\frac{dX_{p,r}}{dt} = \frac{CL_{tt} \times Fr}{V_c} \times X_{plasma} - \frac{CL_{ttvr} \times (1 - Frt)}{V_r} \times X_{p,r} - \frac{CL_{ttvr} \times Frt}{V_r} \times X_{p,r} + K_{ga} \times X_{transit,7} \quad (2)$$

$$\frac{dX_{m,r}}{dt} = \frac{CL_{ttvr} \times Frt}{V_r} \times X_{p,r} - \frac{CL_{vrtp}}{V_{rtp}} \times X_{m,r} \quad (3)$$

Clearance from plasma into the tissues were described as fractions of total clearance (CL_{tt}) – with Fv denoting fraction going into vaginal tissue, Fe as fraction going to cervical tissue, and Fr as fraction going into rectal tissue (Equation 1). Rectal tissue amounts ($X_{p,r}$) were described with seven transit compartments leading from depot to describe transit time (Equation 2). Similarly, conversion from parent to metabolite was parameterized as fractions: Fvt for vaginal tissue, Fet for cervical tissue, and Frt for rectal tissue. Using rectal tissue amount ($X_{m,r}$) of metabolite as an example, CL_{ttvr} is total clearance of parent from rectal tissues (Equation 3).

Estimated and fixed parameters are shown in Table 1 along with corresponding IIV and residual variability as well as shrinkage. Off-diagonals were also estimated in the residual variability variance–covariance matrix between the parent and metabolite to account for within-sample correlations. An exponential IIV error model was used:

$$\theta_i = \theta_{typical} \times e^{\eta i} \text{ (individual parameter } \theta \text{ for } i \text{ th individual)}$$

η is normally distributed with mean 0, variance ω^2.

Whereas a proportional residual error model was used:

$$C_{ij}, \text{observed} = C_{ij}, \text{predicted} + C_{ij}, \text{predicted} \times \varepsilon_{ij}$$

(Concentration for i th individual at time j)

ε is normally distributed with mean 0 and variance σ^2.

Off-diagonals in the IIV variance–covariance matrix was implemented between CLtt and V_c; there were no other significant parameter correlations.

Relative standard errors for plasma parameters are shown in Table S2 and are all under 20%. The convergence step for the plasma tenofovir model was only able to work when IIV for K_a was removed.

The goodness of fit plots (Figure 2) show that the model performed well across all concentration ranges and time. The plots are grouped by symbols depicting different matrices and analytes. Plasma (+) is shown in black, vaginal tissue in blue (o), cervical tissue in green (□), and rectal tissue in red (Δ). Closed symbols are the parent species (TFV or FTC), whereas open symbols are the metabolites (TFVdp and FTCtp). There was no significant bias in predictions across all concentration ranges for both TFV (Figure 2a) and FTC (Figure 2b). It was more difficult to fit the metabolites, reflected in the larger residuals of TFVdp (Figure 2a) and FTCtp (Figure 2b). There was no significant prediction bias across time with any compound (Figure 2c,d). Goodness of fit plots of standalone plasma, vaginal, cervical, and rectal have also been provided (Figures S1–S4).

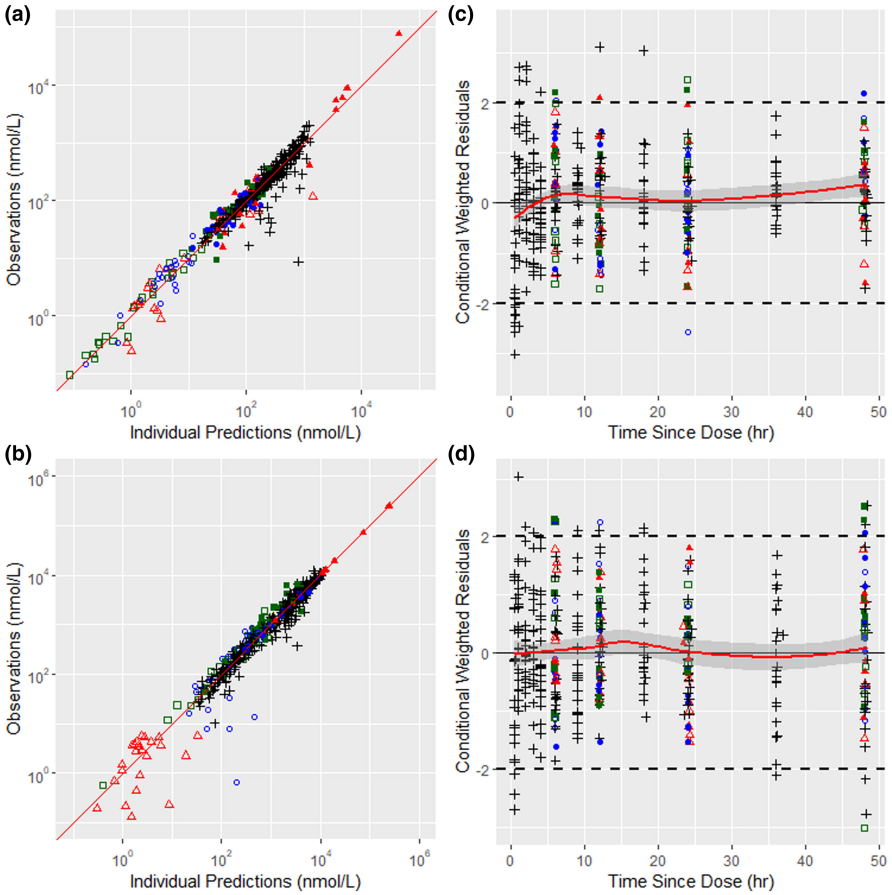

FIGURE 2 Observed vs. predicted show that the model predicts concentrations of TFV (a) and FTC (b) well in plasma (+, black), vaginal tissue (o, blue), cervical tissue (□, green), and rectal tissue (Δ, red) with the Loess line (----) falling along the line of identity. (Parent = closed, metabolite = open symbols.) There is no bias over time in the residuals of TFV (c) and FTC (d). FTC, emtricitabine; TFV, tenofovir.

The model performed well during Monte-Carlo Simulations and was able to capture the observations (Figure 3). In the pcVPC, 17 of 275 (6.2%) of plasma TFV and 14 of 276 (5.1%) of FTC observations were outside the 5%–95% prediction intervals. In the tissues, three of 69 (4.3%) of TFV and five of 69 (7.2%) of TFVdp were outside the 5%–95% CI; five of 68 (11.8%) of FTC and eight of 68 (11.8%) of FTCtp were outside the 5%–95% CI. Additional pcVPC plots for cervical tissues (Figure S5) and TFVdp and FTCtp in vaginal, cervical, and rectal tissues (Figure S6).

A sensitivity analysis was also completed providing additional evidence of consistency in the model through varying select fixed parameters by a degree of magnitude and evaluating the effect on the resulting estimates. Fixed parameters that were tested include volume of distribution of organs and fractions of total clearance. Results after sensitivity analysis showed consistency and proportional changes in related parameters.

DISCUSSION

This model is useful for describing the distribution of TFV/FTC and their respective metabolites (TFVdp/FTCtp) into the female genital tract and rectal tissues. This model is also semi-physiologic, with physiologically relevant parameters used for tissue volumes, as described in the Section 2.[28] There are two advantages to this approach. First, this is a much easier method to simulate with than a full physiologic-based pharmacokinetic (PBPK) model. Second, the parameters developed here are valuable for future full PBPK models.

Linear kinetics was sufficient to describe the pharmacokinetic system. There was no systematic bias in the post hoc parameters (Figure S5), residuals (Figure 2, Figures S1–S4) and pcVPC (Figure 3) by dosing group. This is probably due to the relatively narrow dose range in this study compared to traditional dose-ranging studies.[29] An important significance is that the prediction intervals generated from this model are only relevant within our dose range.

We attempted to estimate as many parameters as possible, even some unidentifiable ones, such as fractions. It was not until we encountered estimation difficulties (such as boundary errors and zero gradient) that we fixed certain parameters (Table 1). For instance, Fet (fraction of parent converted to metabolite in cervical tissue) can be estimated with the TFV dataset but not in the FTC dataset due to lower boundary error. This is not a significant issue because these parameters are not structurally identifiable given the dataset and will not affect the fit. Low shrinkage estimates for two of the metabolite clearance parameters from vaginal and cervical tissues (CL_{vvtp}, CL_{vetp}; Table 1; Figure S7) are likely

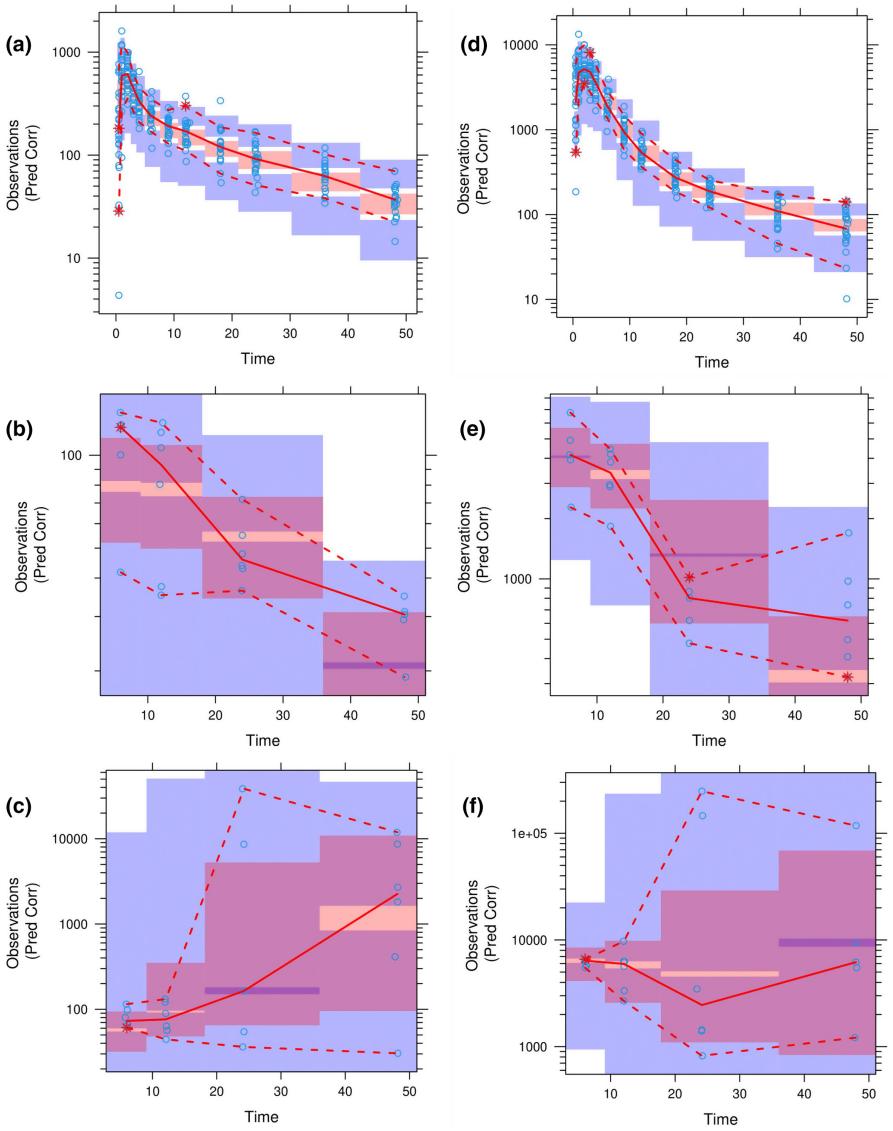

FIGURE 3 The pcVPCs. The solid is the median, dashed is 5%–95% prediction interval, and shades are 95% CI of prediction intervals. There was no bias in plasma TFV (a), vaginal tissue (b), or rectal tissue (c). The model performs similarly well with FTC in plasma (d), vaginal tissue (e), and rectal tissue (f). There was no bias among 50% (+), 100% (◊), and 200% (●) dosing arms. CI, confidence interval; FTC, emtricitabine; pcVPCs, prediction-corrected visual predictive checks; TFV, tenofovir.

due to wide variability in the estimates of these difficult-to-characterize parameters and were retained in the model to consistently apply criteria for removing shrinkage terms. The wide variability in the estimates of these metabolite clearances is also reflected in Figure S6. Tissue samples are difficult to obtain in humans and require complex processing and analysis methods to measure drug concentrations, adding to the inherent variability of metabolite measurements. In peripheral blood mononuclear cells (PBMCs), which can be obtained more frequently and are far more accessible than tissue biopsies, metabolite concentrations also vary considerably, at least partially due to complexities in cell isolation and analytical methods. We and others have observed pcVPCs in PBMC models similar to those seen here for tissues.[8,15,30,31]

We do not have bootstrap results of parameter precision estimates due to the excessively long model run time. Even with parallelization across 24 CPUs on our Linux cluster, the model took over a week to converge; therefore a 100 replicate bootstrap would take 2 years to complete. Regardless, the bootstrap results may not be meaningful due to the relatively few tissue samples we have. We are nonetheless confident with the parameter estimates due to the calculation of reasonable standard errors for the plasma compartment (Table S2). Although extrapolation to the full model was not possible due to the sparsity of tissue and metabolite data, the calculated plasma parameters remained constant through the model development process. Determining whether other estimation algorithms (such as stochastic expectation-maximization[32]) will affect the parameter estimates is an important future consideration for our work.

We also have not implemented covariate models, due to the homogeneity of our population (Table S1). However, incorporating previously published covariate models will allow us to examine the effects of potential covariates on tissue kinetics and extrapolate these data to a heterogeneous population.[11,12,33–36]

Additionally, plasma metabolite data were collected but were not modeled here, as the purpose of this model was to describe drug disposition at mucosal tissues. Adding plasma metabolite data would have resulted in a more complicated model not helped by the already limited tissue metabolite data. Modeling using the PBMC metabolite data from this study has been performed to explore prevention of HIV transmission via intravenous drug use.[31]

To our knowledge, the present model represents the most comprehensive mathematical model describing the pharmacokinetics of tenofovir disoproxil fumarate and FTC. Our model simultaneously predicts the exposure of tenofovir, FTC, and their active metabolites in the blood and the mucosal tissue compartments exposed to HIV during sexual transmission, the female genital and lower GI tracts.

This model has been combined with in vitro efficacy targets to investigate the number of doses required for effective PrEP in different tissues, helping illuminate possible causes of the disparity of minimum effective doses between men and women, including for event-driven dosing.[18,37] This proof of concept gives credence that this model can be a powerful tool for PrEP clinical trial simulations to explore exposure from different dosing strategies for HIV PrEP in the different tissue sites exposed to HIV as well as being used to inform possible optimal/minimal doses required for prevention in different patient populations. Indeed, our results suggesting that four doses per week are sufficient to protect rectal tissues, which lower FGT protection requires consistent daily dosing are consistent with the combined analysis of the HPTN 083/084 clinical studies,[38] and several clinical trials using both oral and vaginal administration.[39]

AUTHOR CONTRIBUTIONS

E.L., J.B.D., M.L.C., and A.D.M.K. wrote the manuscript. A.D.M.K. designed the research. M.L.C., C.S., and N.W. performed the research. E.L., J.B.D., M.L.C., C.S., and N.W. analyzed the data.

ACKNOWLEDGMENTS

The authors acknowledge the contributions of Kuo H. Yang, PharmD, MS, who performed initial model fitting/simulations; Heather M.A. Prince, PA-C, who conducted the clinical study; and Stephanie Malone, BS, who performed sample analysis to earlier iterations of this work. We would also like to sincerely thank the study participants who volunteered their time and effort to make this research possible.

FUNDING INFORMATION

This work was supported by the National Institute of Allergy and Infectious Diseases (grant number U01 AI09503), the Centers for AIDS Research (grant number CFAR P30 AI50410), and the National Institute of General Medical Sciences (grant number 5T32GM086330). The content is solely the responsibility of the authors and does not necessarily represent the official views of the supporting agencies listed above.

CONFLICT OF INTEREST STATEMENT

A.K. and her laboratory are part of the study teams for CAPRISA 004 and 008, FACTS 001, MTN 006, HPTN 066, FEM-PrEP, and CONRAD 113, 114, and 117. Grant funding from Gilead has been received by UNC and A.K. All other authors declared no competing interests for this work.

ORCID

Erick Leung https://orcid.org/0000-0002-3753-1900
Mackenzie L. Cottrell https://orcid.org/0000-0002-0291-5111
Angela D. M. Kashuba https://orcid.org/0000-0002-9171-8493
Julie B. Dumond https://orcid.org/0000-0002-3500-5819

REFERENCES

1. Thigpen MC, Kebaabetswe PM, Paxton LA, et al. Antiretroviral preexposure prophylaxis for heterosexual HIV transmission in Botswana. *N Engl J Med*. 2012;367:423-434.
2. Baeten JM, Donnell D, Ndase P, et al. Antiretroviral prophylaxis for HIV prevention in heterosexual men and women. *N Engl J Med*. 2012;367:399-410.
3. Van Damme L, Corneli A, Ahmed K, et al. Preexposure prophylaxis for HIV infection among African women. *N Engl J Med*. 2012;367:411-422.
4. Marrazzo JM, Ramjee G, Richardson BA, et al. Tenofovir-based preexposure prophylaxis for HIV infection among African women. *N Engl J Med*. 2015;372:509-518.
5. Anderson PL, Glidden DV, Liu A, et al. Emtricitabine-tenofovir concentrations and pre-exposure prophylaxis efficacy in men who have sex with men. *Sci Transl Med*. 2012;4:151ra125.
6. Grant RM, Anderson PL, McMahan V, et al. Uptake of pre-exposure prophylaxis, sexual practices, and HIV incidence in men and transgender women who have sex with men: a cohort study. *Lancet Infect Dis*. 2014;14:820-829.
7. Jullien V, Tréluyer JM, Rey E, et al. Population pharmacokinetics of tenofovir in human immunodeficiency virus-infected patients taking highly active antiretroviral therapy. *Antimicrob Agents Chemother*. 2005;49:3361-3366.
8. Baheti G, Kiser JJ, Havens PL, Fletcher CV. plasma and intracellular population pharmacokinetic analysis of tenofovir in HIV-1-infected patients. *Antimicrob Agents Chemother*. 2011;55:5294-5299.
9. Dumond JB, Nicol MR, Kendrick RN, et al. Pharmacokinetic modelling of efavirenz, atazanavir, lamivudine and tenofovir in the female genital tract of HIV-infected pre-menopausal women. *Clin Pharmacokinet*. 2012;51:809-822.
10. Hirt D, Urien S, Rey E, et al. Population pharmacokinetics of emtricitabine in human immunodeficiency virus type 1-infected pregnant women and their neonates. *Antimicrob Agents Chemother*. 2009;53:1067-1073.

11. Madrasi K, Burns RN, Hendrix CW, Fossler MJ, Chaturvedula A. Linking the population pharmacokinetics of tenofovir and its metabolites with its cellular uptake and metabolism. *CPT Pharmacometrics Syst Pharmacol*. 2014;3:e147.
12. Burns RN, Hendrix CW, Chaturvedula A. Population pharmacokinetics of tenofovir and tenofovir-diphosphate in healthy women. *J Clin Pharmacol*. 2015;55:629-638.
13. Quashie PK, Mesplède T, Han YS, et al. Characterization of the R263K mutation in HIV-1 integrase that confers low-level resistance to the second-generation integrase strand transfer inhibitor dolutegravir. *J Virol*. 2012;86:2696-2705.
14. Chaturvedula A, Fossler MJ, Hendrix CW. Estimation of tenofovir's population pharmacokinetic parameters without reliable dosing histories and application to tracing dosing history using simulation strategies. *J Clin Pharmacol*. 2014;54:150-160.
15. Greene SA, Chen J, Prince HMA, et al. Population modeling highlights drug disposition differences between tenofovir alafenamide and tenofovir disoproxil fumarate in the blood and semen. *Clin Pharmacol Ther*. 2019;106(4):821-830. doi:10.1002/cpt.1464
16. Reigner BG, Williams PEO, Patel IH, Steimer JL, Peck C, van Brummelen P. An evaluation of the integration of pharmacokinetic and pharmacodynamic principles in clinical drug development. Experience within Hoffmann La Roche. *Clin Pharmacokinet*. 1997;33:142-152.
17. Olson SC, Bockbrader H, Boyd RA, et al. Impact of population pharmacokinetic-pharmacodynamic analyses on the drug development process: experience at Parke-Davis. *Clin Pharmacokinet*. 2000;38:449-459.
18. Cottrell ML, Yang KH, Prince HM, et al. A translational pharmacology approach to predicting outcomes of preexposure prophylaxis against HIV in men and women using tenofovir disoproxil fumarate with or without emtricitabine. *J Infect Dis*. 2016;214:55-64.
19. R Core Team R. *A Language and Environment for Statistical Computing*. 2013. http://www.r-project.org/
20. Wickham H. *ggplot2: Elegant Graphics for Data Analysis*. Springer New York; 2009. http://had.co.nz/ggplot2/book
21. Wickham H, Francois R. dplyr: A grammar of data manipulation. 2015. http://cran.r-project.org/package=dplyr
22. Wickham H. tidyr: Easily Tidy Data with spread() and gather() Functions. 2014. http://cran.r-project.org/package=tidyr
23. Guiastrennex B. xpose: Diagnostics for Pharmacometric Models. 2021. https://cran.r-project.org/web/packages/xpose/index.html
24. Hénin E, Bergstrand M, Standing JF, Karlsson MO. A mechanism-based approach for absorption modeling: the gastro-intestinal transit time (GITT) model. *AAPS J*. 2012;14:155-163.
25. Bergstrand M, Hooker AC, Wallin JE, Karlsson MO. Prediction-corrected visual predictive checks for diagnosing nonlinear mixed-effects models. *AAPS J*. 2011;13:143-151.
26. Canty A, Ripley BD. boot: Bootstrap R (S-Plus) Functions. 2015.
27. Davison AC, Hinkley D. *V Bootstrap Methods and Their Applications*. Cambridge University Press; 1997. http://statwww.epfl.ch/davison/BMA/
28. Fedoriw G. Personal Correspondance. 1. 2014.
29. Kearney BP, Flaherty JF, Shah J. Tenofovir disoproxil fumarate: clinical pharmacology and pharmacokinetics. *Clin Pharmacokinet*. 2004;43:595-612.
30. Dumond JB, Collins JW, Cottrell ML, et al. p16INK4a, a senescence marker, influences tenofovir/emtricitabine metabolite disposition in HIV-infected subjects. *CPT Pharmacometrics Syst Pharmacol*. 2019;6(2):120-127.
31. Garrett KL, Chen J, Maas BM, et al. A pharmacokinetic/pharmacodynamic model to predict effective HIV prophylaxis dosing strategies for people who inject drugs. *J Pharmacol Exp Ther*. 2018;367(2):245-251. doi:10.1124/jpet.118.251009
32. Chan PLS, Jacqmin P, Lavielle M, McFadyen L, Weatherley B. The use of the SAEM algorithm in MONOLIX software for estimation of population pharmacokinetic-pharmacodynamic-viral dynamics parameters of maraviroc in asymptomatic HIV subjects. *J Pharmacokinet Pharmacodyn*. 2011;38:41-61.
33. Punyawudho B, Thammajaruk N, Thongpeang P, et al. Population pharmacokinetics of tenofovir in HIV/HBV co-infected patients. *Int J Clin Pharmacol Ther*. 2015;53:947-954. doi:10.5414/CP202386
34. Hu C-Y, Liu YM, Liu Y, et al. Pharmacokinetics and tolerability of tenofovir disoproxil fumarate 300 mg once daily: an open-label, single- and multiple-dose study in healthy Chinese subjects. *Clin Ther*. 2013;35:1884-1889.
35. Valade E, Tréluyer JM, Bouazza N, et al. Population pharmacokinetics of emtricitabine in HIV-1-infected adult patients. *Antimicrob Agents Chemother*. 2014;58:2256-2261.
36. Wahl A, Ho PT, Denton PW, et al. Predicting HIV preexposure prophylaxis efficacy for women using a preclinical pharmacokinetic-pharmacodynamic in vivo model. *Sci Rep*. 2017;7:41098.
37. Dumond JB, Cottrell ML, Symonds AE, Sykes C, White N, Kashuba AD. Predicted success of PreP Users' preferred non-daily tenofovir/emtricitabine regimens. *Science Spotlight*, CROI 2021. February 2021.
38. Anderson PL, Marzinke MA, Glidden DV, et al. Updating the adherence-response for oral emtricitabine/tenofovir disoproxil fumarate for human immunodeficiency virus pre-exposure prophylaxis among cisgender women. *Clin Infect Dis*. 2023;76(10):1850-1853.
39. Garcia-Cremades M, Vučićević K, Hendrix CW, et al. Characterizing HIV-preventive, plasma tenofovir concentrations – a pooled participant-level data analysis from human immunodeficiency virus preexposure prophylaxis clinical trials. *Clin Infect Dis*. 2022;75(11):1873-1882.

SUPPORTING INFORMATION

Additional supporting information can be found online in the Supporting Information section at the end of this article.

How to cite this article: Leung E, Cottrell ML, Sykes C, White N, Kashuba ADM, Dumond JB. A multicompartment population PK model to predict tenofovir and emtricitabine mucosal tissue concentrations for HIV prevention. *CPT Pharmacometrics Syst Pharmacol*. 2023;12:1922-1930. doi:10.1002/psp4.13042